BBA - Molecular Basis of Disease 1865 (2019) 56–62

Contents lists available at ScienceDirect

BBA - Molecular Basis of Disease

journal homepage: www.elsevier.com/locate/bbadis

Nr5a1-Cre-mediated *Tspo* conditional knockout mice with low growth rate and prediabetes symptoms – A mouse model of stress diabetes

Jinjiang Fan[a,b], Enrico Campioli[a,b], Vassilios Papadopoulos[a,b,c,*]

[a] The Research Institute of the McGill University Health Centre, Montreal, Quebec, Canada
[b] Department of Medicine, McGill University, Montreal, Quebec, Canada
[c] Department of Pharmacology and Pharmaceutical Sciences, School of Pharmacy, University of Southern California, Los Angeles, CA, United States

ARTICLE INFO

Keywords:
Tspo
Nr5a1-Cre
Conditional knockout
Low growth rate
Prediabetes
Hyperglycemia

ABSTRACT

Translocator protein (TSPO) is a high-affinity cholesterol- and drug-binding mitochondrial protein. Nuclear receptor subfamily 5 group A member 1 or steroidogenic factor 1 (*Nr5a1*)-Cre mice were previously used to generate steroidogenic cell-specific *Tspo* gene conditional knockout (cKO) mice. TSPO-depleted homozygotes showed no response to adrenocorticotropic hormone (ACTH) in stimulating adrenal cortex corticosterone production but showed increased epinephrine synthesis in the medulla. No other phenotype was observed under normal growth conditions. During these studies, we noted that pairing two cKO mice resulted in the generation of small pups. These pups showed low growth rate at weaning, which has been linked to the development of type 2 diabetes (T2D) in adulthood. Experimental verification of T2D symptoms via blood testing of the adult mice, including glycated hemoglobin and insulin C-peptide measurements, showed that these *Tspo* cKO mice exhibited sustained hyperglycemia, a sign of prediabetes, likely due to the augmentation of hepatic glucose production mediated by the increased epinephrine. We also observed increased expression of the *S100a8* gene, which is upregulated after chronic glucose stimulation. Taken together, the observed prediabetes phenotype and lack of response to ACTH indicate that *Tspo* cKO mice (*Nr5a1*-Cre$^{+/-}$, *Tspo*$^{fl/fl}$) could provide a useful model to study the link between diabetes and stress.

1. Introduction

The outer mitochondrial membrane translocator protein (TSPO), a high-affinity cholesterol- and drug-binding protein, possesses multiple biological activities, including mitochondrial cholesterol transport and steroid hormone biosynthesis, porphyrin transport and heme synthesis, cell proliferation, and apoptosis [1]. TSPO is also involved in anion transport, which is likely related to the regulation of mitochondrial membrane potential [1,2]. These functions were elucidated by either controlling protein expression or using drug ligands. Recent studies have shown that TSPO may also serve as a drug target for diabetes and obesity by regulating glucose metabolism and glucose uptake in adipose tissue [3]. In addition, TSPO ligands have been shown to prevent hepatosteatosis and glucose intolerance in mice with high-fat diet-induced obesity [4]. Therefore, modulation of TSPO function via drug ligands or by loss-of-function to regulate glucose homoeostasis and energy production may be effective in treating these two pathological manifestations of mitochondrial metabolic dysregulation [5].

We previously showed that nuclear receptor subfamily 5 group A member 1 (*Nr5a1*, also known as steroidogenic factor 1; *Sf-1*)-Cre mediated steroidogenic cell-specific *Tspo* conditional knockout (cKO) resulted in altered neutral lipid deposition, reduced circulating plasma corticosterone levels in response to adrenocorticotropic hormone (ACTH) stimulation, and increased production of epinephrine, a stress response mediator [6]. This lipid accumulation phenotype is similar to that of steroidogenic acute regulatory protein (*Star*) KO mice, in which the accumulation of lipid droplets in the adrenal cortex is also linked to reduced steroid formation [7]. The physiological significance of increased epinephrine in steroidogenic cells of *Tspo* cKO mice is unknown. We hypothesize that the increased epinephrine production serves as an adaptive mechanism in the presence of *Tspo* deficiency [6].

Abbreviations: ACTH, adrenocorticotropic hormone; cHE, conditional knockout heterozygote; cHO, conditional knockout homozygote; cKO, conditional knockout; Cpeb4, cytoplasmic polyadenylation element-binding protein 4; Cyp1b1, cytochrome P450, family 1, subfamily b, polypeptide 1; ELISA, enzyme-linked immunosorbent assay; GHbA1c, glycated hemoglobin A1c; HDL, high-density lipoprotein; Hprt, hypoxanthine-guanine phosphoribosyltransferase; Igf2r, insulin-like growth factor 2 receptor; Nr5a1, nuclear receptor subfamily 5 group A member 1; Sf-1, steroidogenic factor 1; S100a8, S100 calcium-binding protein A8; Sepp1, selenoprotein P; Star, steroidogenic acute regulatory protein; T2D, type 2 diabetes; TSPO, translocator protein; WT, wild type

* Corresponding author at: Department of Pharmacology and Pharmaceutical Sciences, School of Pharmacy, University of Southern California, Los Angeles CA, United States
E-mail address: vpapadop@usc.edu (V. Papadopoulos).

https://doi.org/10.1016/j.bbadis.2018.10.022
Received 12 July 2018; Received in revised form 10 October 2018; Accepted 16 October 2018
Available online 18 October 2018

Epinephrine, which plays an important role in the fight-or-flight response, is one of the main counter-regulatory hormones to insulin, inhibiting insulin secretion and increasing gluconeogenesis and glycogenolysis in the liver, thus boosting blood glucose levels [8–10]. We report herein that *Tspo* cKO mice frequently showed slow growth at the weaning and young adult stages. As adults, these mice tended to develop a type 2 diabetes (T2D) phenotype, exhibiting sustained high blood glucose or hyperglycemia, which is the hallmark of prediabetes.

2. Materials and methods

2.1. Generation of Tspo cKO mice

Generation of the steroidogenic cell-specific *Tspo* cKO mice (homozygous cHO: *Nr5a1*-Cre$^{+/-}$, *Tspo*$^{fl/fl}$; heterozygous cHE: *Nr5a1*-Cre$^{+/-}$, *Tspo*$^{fl/+}$) was previously described [5]. In brief, *Tspo* cHO mice (*Nr5a1*-Cre$^{+/-}$, *Tspo*$^{fl/fl}$) were produced by crossing heterozygous *Tspo* cHE mice (*Nr5a1*-Cre$^{+/-}$, *Tspo*$^{fl/+}$) with homozygous *Tspo* floxed mice (*Nr5a1*-Cre$^{-/-}$, *Tspo*$^{fl/fl}$) (see Table 1). Both the *Tspo* floxed and *Nr5a1*-Cre mouse lines were maintained by crossing with wild type (WT) C57BL/6J mice from the Jackson Laboratory. *Tspo* cHO mice were generated through two rounds of crossing: homozygous *Tspo* floxed mouse (*Nr5a1*-Cre$^{-/-}$, *Tspo*$^{fl/fl}$) × Cre-positive mouse (*Nr5a1*-Cre$^{+/-}$, *Tspo*$^{+/+}$), and then crossing with the resulting heterozygous *Tspo* cHE mice (*Nr5a1*-Cre$^{+/-}$, *Tspo*$^{fl/+}$). WT crossings (*Nr5a1*-Cre$^{+/-}$ or *Tspo*$^{fl/fl}$ floxed lines) served as control (s). Two cHO mice were mated to produce pups for body weight measurements at the weaning stage (21–26 days) and young adult stage (35–45 days), and the growth rate was calculated by dividing weight by actual days after birth; WT mice served as control(s). Animals were handled according to protocols approved by the McGill University Animal Care and Use Committee.

2.2. Immunofluorescence staining and microscopy

Routine immunofluorescence staining of cryosections of adrenal gland, testis, and ovary tissues was performed as previously described [6]. Briefly, tissue cryosections were fixed in 4% paraformaldehyde, permeabilized with 0.1% Triton X, blocked with 1% bovine serum albumin containing 1% donkey serum, and incubated in primary rabbit anti-TSPO monoclonal antibody (clone EPR5384, ab109497; Abcam, Toronto, ON, Canada), followed by secondary donkey anti-rabbit IgG (H + L) antibody conjugated with Alexa Fluor® 546 (Thermo Fisher, Burlington, ON, Canada). Nuclei were counterstained using UltraCruz® aqueous mounting medium containing 4′,6-diamidino-2-phenylindole (Santa Cruz Biotechnology Inc., Dallas, TX, USA). Microscopy was performed using Olympus FV1000 and Zeiss LSM 780 confocal laser scanning microscopes, and epifluorescence imaging was performed with an inverted Olympus microscope. All images were analyzed using ImageJ software (National Institutes of Health, Bethesda, MD, USA).

2.3. Serum biochemical profile, glycated hemoglobin A1c test, and insulin C-peptide measurement

We collected blood samples (sufficient to obtain 250 µl serum) from cHO and WT adult mice (~12 months old) for serum biochemical analysis, which was carried out at the Diagnostic and Research Support Service, Comparative Medicine and Animal Resources Centre, McGill University. At the terminal stage of the study, we collected whole blood by cardiac puncture and then harvested the liver, pancreas, adipose, thigh muscle, testis/ovary, and adrenal glands. We determined levels of glycated hemoglobin A1c (GHbA1c) and insulin C-peptide using a Mouse GHbA1c ELISA Kit (MG0329; NeoScientific, Cambridge, MA, USA) and Mouse Insulin C-Peptide ELISA Kit (Competitive EIA)(LS-F25003; LifeSpan BioSciences, Inc., Seattle, WA, USA), respectively, in accordance the manufacturers' instructions. Absorbance was read at 450 nm using a VICTOR™ X5 Multilabel Plate Reader (PerkinElmer Inc., Waltham, MA, USA).

Table 1
List of mice used and their corresponding genotypes.

Abbreviation	Full name	Genotype
WT	C57BL/6J mouse (wild type)	*Nr5a1*-Cre$^{-/-}$, *Tspo*$^{+/+}$
Nr5a1-Cre	*Nr5a1*-Cre-positive mouse (wild type)	*Nr5a1*-Cre$^{+/-}$, *Tspo*$^{+/+}$
Tspo cKO	*Nr5a1*-Cre mediated *Tspo* conditional knockout	*Nr5a1*-Cre$^{+/-}$, *Tspo*$^{+/fl}$ and *Nr5a1*-Cre$^{+/-}$, *Tspo*$^{fl/fl}$
cHE	*Nr5a1*-Cre-positive, heterozygous floxed *Tspo* alleles	*Nr5a1*-Cre$^{+/-}$, *Tspo*$^{+/fl}$
cHO	*Nr5a1*-Cre-positive, homozygous floxed *Tspo* alleles	*Nr5a1*-Cre$^{+/-}$, *Tspo*$^{fl/fl}$

2.4. Microarray analysis and real-time PCR

2.4.1. Human gene expression

Microarray data of gene expression in liver biopsies of human subjects with or without type 2 diabetes [11] were retrieved from NCBI GEO database (accession no.: GSE23343) [11]. The data were reanalyzed using FlexArray software (version 1.61; http://genomequebec.mcgill.ca/FlexArray) and normalized by robust multiarray average. Differences in gene expression between hyperglycemic patients and controls were visualized by using volcano plots (see Fig. S1), which showed that the following genes were differentially regulated in hyperglycemic patients: S100 calcium-binding protein A8 (*S100a8*), cytoplasmic polyadenylation element-binding protein 4 (*Cpeb4*), cytochrome P450, family 1, subfamily b, polypeptide 1 (*Cyp1b1*), insulin-like growth factor 2 receptor (*Igf2r*), and selenoprotein P (*Sepp1*).

2.4.2. Mouse gene expression

The mouse orthologs of genes found to be highly regulated in hyperglycemic patients (see Section 2.4.1) were analyzed in our mouse liver samples by real-time PCR. Total RNA was extracted using TRIzol Reagent (Thermo Fisher Scientific). Purity of the RNA samples was determined by NanoDrop spectrophotometer, and those with 260/280 and 260/230 ratios of 1.8–2.0 and 2.0–2.2, respectively, were deemed acceptable for further analysis. After treating the RNA samples with a DNA-free DNA Removal Kit (Thermo Fisher Scientific) and diluting to 100 ng/µl using DNase/RNase-free water, cDNA was synthesized using the Transcriptor First Strand cDNA Synthesis Kit (Roche Applied Science), according to manufacturer's instructions. The resulting cDNA samples were diluted with nuclease-free water and analyzed by real-time PCR using SYBR Green dye and a LightCycler 480 system (Roche Applied Science) as previously described [27]. Target genes were normalized to hypoxanthine-guanine phosphoribosyltransferase (*Hprt*) to correct for differences in template cDNA quantities.

We used the following primer sets: S100A8-R: AGTGTCCTCAGTTTGTGCAG and S100A8-F: GAGATGCCACACCCACTTT for *S100a8*; Cpeb4-R: GGTGGATTG CCTCCTGATATT and Cpeb4-F: AGATTTGCTCTCTGCCTTATGA for *Cpeb4*; Cyp1b1-R: CTGCCACTATTACGGACATCTT and Cyp1b1-F: GCCTGAACATCCGG GTATC for *Cyp1b1*; Igf2r-R: GCCTACAAGTGCTATCTGTATGT and Igf2r-F: GGT GTTGAATTCCAGGAGTGA for *Igf2r*; Sepp1-R: GCTAAACTCAGAGGGCAAAGT and Sepp1-F: TATGCGCAGGTCTTCCAATC for *Sepp1*; and Hprt-R: GCGTCGTGA TTAGCGATGATGAAC and Hprt-F: GAGCAAGTCTTTCAGTCCTGTCCA for *Hprt*.

2.5. Statistical analysis

Statistical analyses were performed using GraphPad Prism 5.02 software. The significance of the results was determined using Student's *t*-test and F-test for equality of variance; $p < 0.05$ was considered significant.

3. Results

3.1. Low growth rate of pups generated by crossing two cHO mice (Nr5a1-Cre$^{+/-}$, Tspo$^{fl/fl}$)

During the characterization of the steroidogenic cell-specific *Tspo* cKO mice (*Nr5a1*-Cre$^{+/-}$, *Tspo*$^{+/fl}$ and *Nr5a1*-Cre$^{+/-}$, *Tspo*$^{fl/fl}$), we observed that pairing two cHO mice from the same litter produced extra small pups (Fig. 1A). The extra small mice were homozygous (cHO, *Nr5a1*-Cre$^{+/-}$, *Tspo*$^{fl/fl}$), and growth rates at the weaning stage (21–26 days) and young adult stage (35–45 days) were significantly lower than those of WT mice (*Nr5a1*-Cre$^{-/-}$, *Tspo*$^{+/+}$) (Fig. 1B). In contrast, the growth rates of small WT pups from the cHO pairing did not differ significantly from those of normal WT mice from control pairing at either the weaning and or young adult stage (Fig. 1B). Results of immunostaining showed that TSPO expression was considerably lower in the adrenal cortex, testes, and

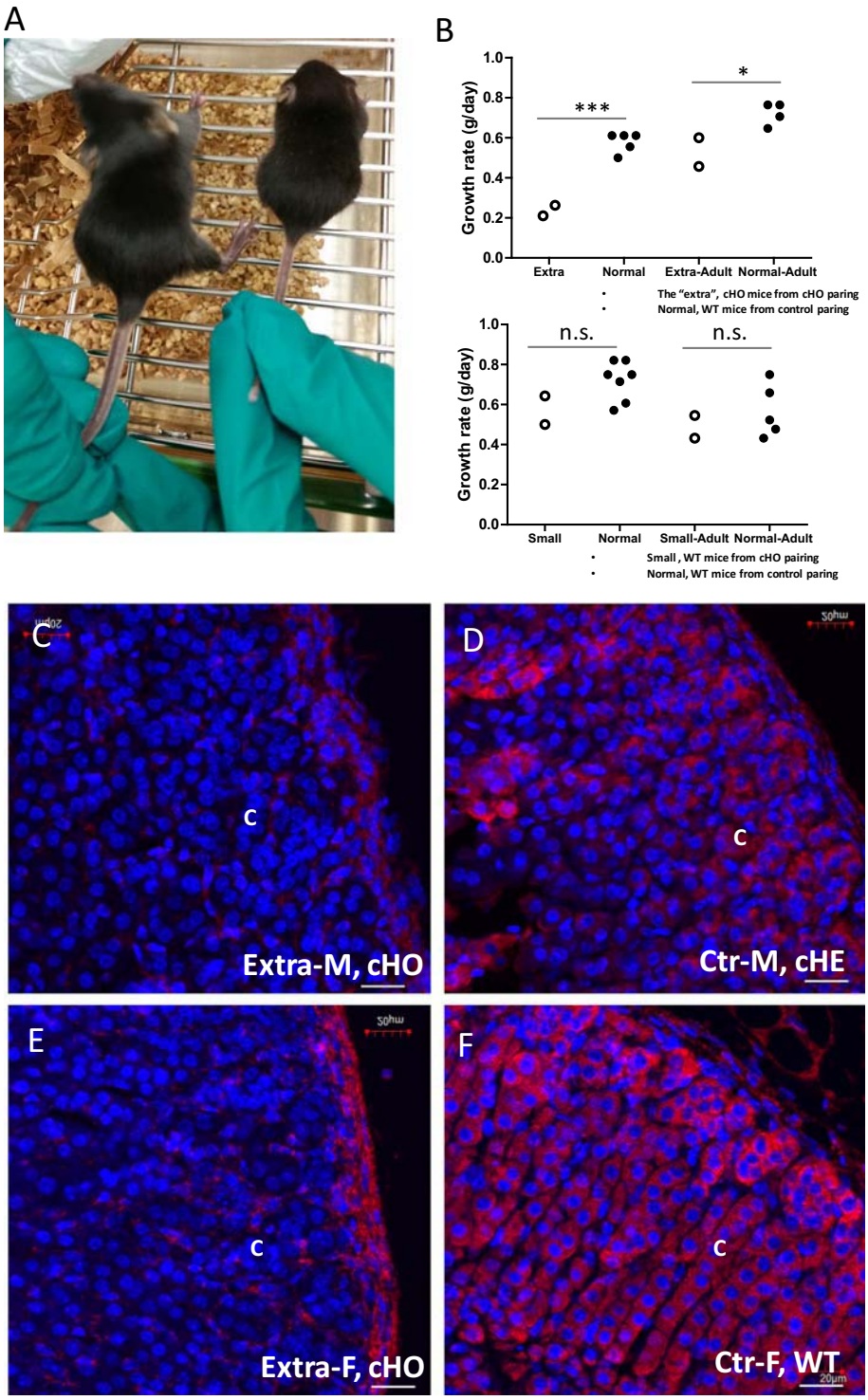

Fig. 1. Extra small pups were produced by a pairing of *Tspo* cHO × cHO mice. (A) Comparison of the same age pups with a size noticeably smaller (right) than that of WT (left). (B) Growth rate (g/day) of pups and young adult mice from the *Tspo* cHO pairing vs. WT control pairing. Upper panel, left: Extra (open circle, extra small cHO pups from *Tspo* cHO pairing) vs. Normal (solid circle, WT pups from WT control pairing) at the weaning stage; upper panel, right: same mice at the young adult stage. Lower panel, left: Small (open circle, WT genotype mice from *Tspo* cHO pairing) vs. Normal (solid circle, WT pups from WT control pairing) at the weaning stage; lower panel, right: same mice at the young adult stage. ***$p < 0.001$; *$p < 0.05$; n.s., not significant (Student's *t*-test, n = 2–7 mice/group); error bars represent SEM. (C–F) Immunofluorescence staining of TSPO in the adrenal gland of (C) extra small male *Tspo* cHO mice, (D) control cHE male mice, (E) extra small female *Tspo* cHO mice, and (F) control WT female mice (F). C, cortex; Ctr, control. Scale bar = 20 μm.

ovaries of the cKO mice (Figs. 1C, E, S2A, S2C, S3A, S3C, S4A, and S4C) compared with corresponding tissues of WT mice (Figs. 1D, F, S2B, S2D, S3B, S3D, S4B, and S4D), as we previously reported [6].

To understand the lower growth rates of *Tspo* cKO mice, we paired the sire and dam of the extra small mice with young WT mice. We observed all the litter size is within 6–8 pups (Fig. 2A), but female pups produced by the dam had significantly higher growth rates (Fig. 2B). In contrast, pups produced by the sire had growth rates similar to those of pups from the other cHO pairings (approximately 0.4 g/day) (Fig. 2C). Subsequently, we did not observe extra small pups from three additional cHO pairings (*Nr5a1*-Cre$^{+/-}$, *Tspo*$^{fl/fl}$ × *Nr5a1*-Cre$^{+/}$

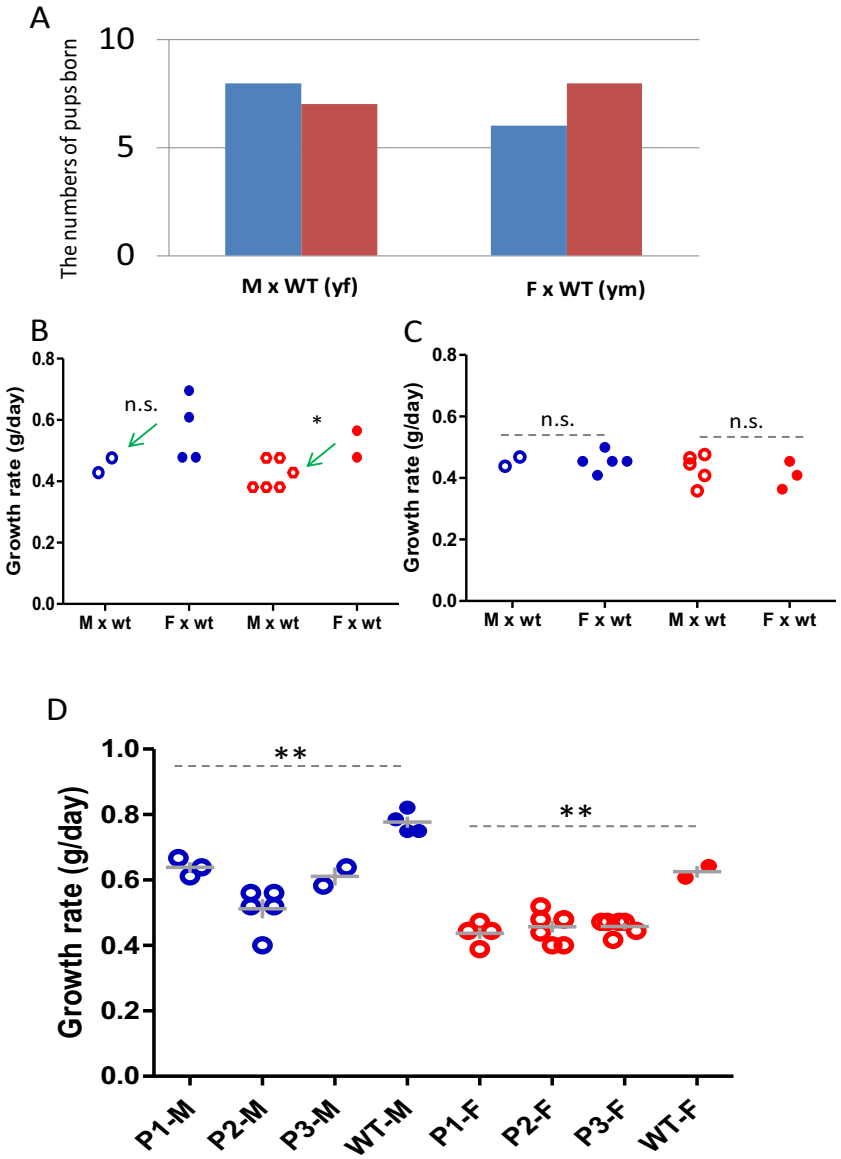

Fig. 2. Cross between parents producing extra small pups, small pups, and WT pups with young adult WT mice. (A) The number of pups from the sire of the extra small pups (M) crossed with a young WT female (WT (yf)) and from the dam of the extra small mice (F) crossed with a young WT male (WT (ym)). Blue, male pups; red, female pups. (B) Growth rate of one litter from the pairing shown in (A). Open circle, pups (male in blue and female in red) from cHO male × WT female pairing; solid circles, pups (male in red and female in blue) from cHO female × WT male pairing. Green arrow, indicates the trend of slow growth of the pups. (C) Growth rates of other cHO and WT mouse pairing as controls. Open circle, pups (male and female) from cHO male × WT female pairing; solid circle, pups (male and female) from cHO female × WT male pairing. *$p < 0.05$; n.s., not significant. (D) Growth rates of pups (~1-month-old) from three pairs of *Tspo* cHO mice (P1 to P3) and WT mice. Male pups (P1-M, P2-M, P3-M, and WT-M) and female pups (P1-F, P2-F, P3-F, and WT-F) were compared, separately. Open circle, pups from cHO pairings; solid circle, pups from WT pairing. **$p < 0.01$ (Student's *t*-test; n = 2–6/each group); error bars represent SEM.

$^{-}$, *Tspo*$^{fl/fl}$), but the growth rates of all offspring were significantly lower than pups from WT pairings (Fig. 2D). These findings show that although the generation of the extra small mice from cKO pairings was an occasional phenomenon, a visible phenotype of slow growth after *Tspo* conditional genetic depletion was common [6].

3.2. Hyperglycemia in the cKO mice

To gain further insight into the low growth rate of cKO mice (*Nr5a1*-Cre$^{+/-}$, *Tspo*$^{+/fl}$ and *Nr5a1*-Cre$^{+/-}$, *Tspo*$^{fl/fl}$), we analyzed serum biochemistry profiles. Compared with WT mice, free cholesterol and serum glucose levels were significantly higher in male cKO mice but not in female cKO mice (Fig. 3A, B). However, high-density lipoprotein (HDL) and triglyceride levels did not differ significantly between cKO mice and WT mice (Fig. 3C, D). The increased free cholesterol after TSPO conditional depletion is consistent with our previous findings of abnormal cholesterol metabolism and its use in steroid or bile acid biosynthesis, as indicated by the accumulation of neutral lipids [6,12]. The sustained high blood glucose levels indicated prediabetes.

To confirm these findings, we measured the GHbA1c and insulin C-peptide levels. The results showed that GHbA1c levels were significantly higher in male cKO (cHE and cHO) mice compared with male WT mice (Fig. 3E). In addition, insulin C-peptide levels were only significantly increased in male cHE mice (Fig. 3F). Taken together, these results suggest that *Nr5a1*-Cre mediated steroidogenic cell-specific TSPO depletion results in hyperglycemia.

3.3. Upregulation of genetic markers of T2D in cKO mice

Hyperglycemia in patients with T2D results from the development of insulin resistance in target tissues, leading to the loss of insulin secretion [13]. Glucose-induced changes in hepatic gene expression in hyperglycemic patients have been

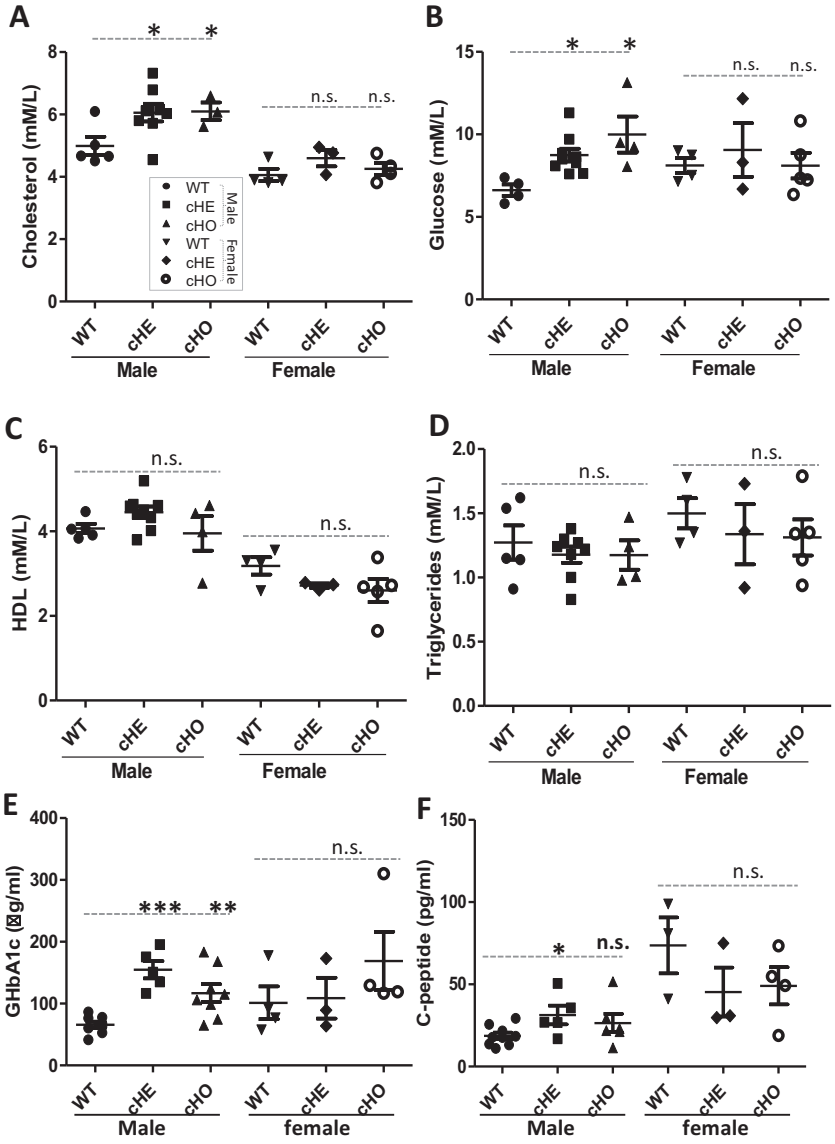

Fig. 3. Hyperglycemia in *Tspo* cKO 1-year-old adult mice. (A–D). Serum biochemistry profiles of *Tspo* cHO mice (*Nr5a1*-Cre$^{+/-}$, *Tspo*$^{fl/fl}$) and cHE mice (*Nr5a1*-Cre$^{+/-}$, *Tspo*$^{+/fl}$) vs. WT mice. (A–B) Free cholesterol and blood glucose levels of male *Tspo* cKO mice (cHO and cHE) were higher than those of male WT mice. (C–D) HDL and triglyceride levels did not differ between *Tspo* cKO and WT mice. *p < 0.05; n.s., not significant (Student's *t*-test, n = 4–8/each group). (E–F) Serum GHbA1c and insulin C-peptide of *Tspo* cKO mice (cHO and cHE) vs. WT mice, as determined by ELISA. ***p < 0.001; **p < 0.01; *p < 0.05, n.s., not significant (Student's *t*-test, n = 8 for WT, 5 for cHE, 8 for cHO; female, n = 5 for WT, 3 for cHE, 4 for cHO); error bars represent SEM. Symbols defined in panel A (inset).

previously reported [11]. Our reanalysis of the original microarray data showed that the following genes were highly regulated in the livers of T2D patients: *SEPP1*, *IGF2R*, *S100A8*, *CPEB4*, and *CYP1B1* (Figs. 4A, S4). Of these genes, only *S100a8* expression was increased in the liver of cKO mice compared with WT mice, as assessed by real-time PCR (Figs. 4B, S5). These data suggest that the high glucose levels in cKO mice are strongly associated with liver expression of *S100a8*, a gene upregulated after chronic glucose stimulation [14].

4. Discussion

In this study, we observed for the first time that steroidogenic cell-specific conditional depletion of *Tspo* leads to hyperglycemia in mice. Since the contradictory reports on the role of TSPO in steroidogenesis, showing either a permissive role or a lack of it in steroid formation, in animal models [6,16] and cell lines [2,17], no other remarkable physiological and/or pathological phenotypes have been reported. Hyperglycemia in mice with steroidogenic cell-specific *Tspo* depletion in this study can be explained by our previous finding that *Tspo* cKO mice have elevated levels of the stress hormone epinephrine [6], which raises blood glucose level [18,19]. Our finding that serum insulin C-peptide level in cHO mice did not differ significantly from that WT mice of suggests that the normal response to insulin is reduced, indicating insulin resistance, which is a characteristic of incipient T2D [13]. Compared with gene expression in hyperglycemic patients with T2D, expression of the mouse orthologs did not show significant changes in cKO mice, except for *S100a8*, which is upregulated after chronic glucose stimulation [14]. Taken together, our data suggest that *Tspo* cKO mice are prediabetic. This observation is in agreement with recent findings showing that TSPO expression is essential for healthy adipocyte function and that TSPO drug ligands improve the metabolic status of adipocytes by regulating glucose homeostasis [3], thereby preventing glucose intolerance in mice with high-fat diet-induced obesity [4].

Further characterization of the *Tspo* cKO mice and their offspring revealed slow growth at the weaning stage, and elevated levels of GHbA1c and free cholesterol, as well as blood glucose, in the adult stage. Low growth rate and sustained hyperglycemia are typical signs of prediabetes leading to T2D. For example, slow growth in the first 6 months after birth in humans is strongly

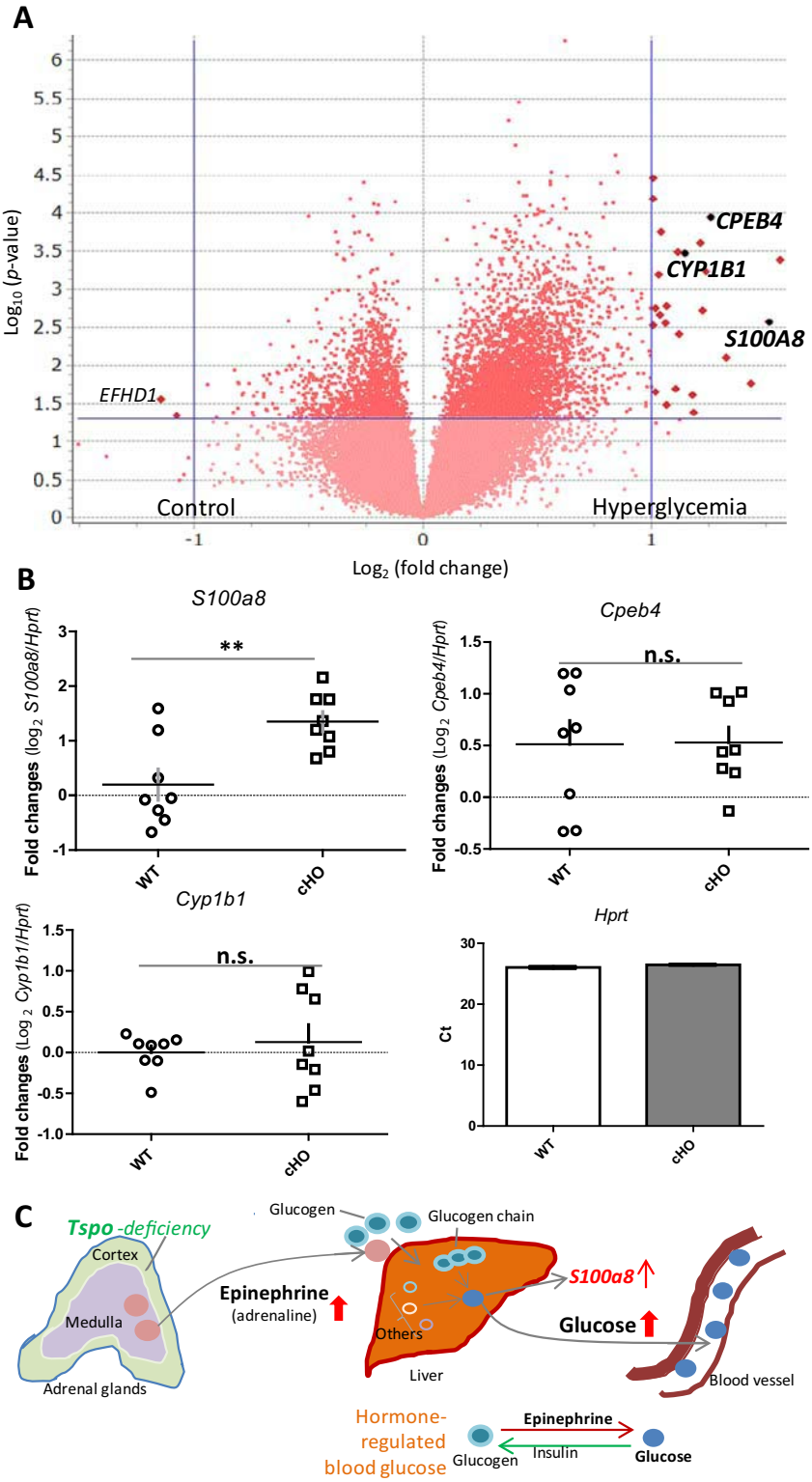

Fig. 4. Expression of hyperglycemia-related genes in the livers of 1-year-old male *Tspo* cKO mice. (A) Volcano plot of liver gene expression in human hyperglycemic patients with T2D vs. controls (NCBI GEO: GSE23343). Upregulated genes associated with hyperglycemia are shown in bold font. (B) Real-time PCR analysis of corresponding mouse orthologs of selected hyperglycemia genes in livers of mice with TSPO deficiency vs. controls. Open circle, WT; open square, cHO. **p < 0.01; Student's *t*-test (n = 7–8/group); error bars represent SEM. (C) Working model of TSPO deficiency leading to hormone-regulated increase in blood glucose level [15]. *Nr5a1*-Cre-mediated *Tspo* cKO in the adrenal gland increases production of epinephrine, leading to increased blood glucose level and *S100a8* expression.

associated with T2D in adulthood [20]. Both nutrition and genetic factors play important roles in this association [21], which is likely related to impaired glucose tolerance [22–25]. In this study, the observed phenotype in the *Tspo* cKO mice was more pronounced in male mice, suggesting a sex-specific trait. As we previously reported, cholesterol stores (lipid droplets) are depleted in *Tspo* cKO mice, suggesting that TSPO affects lipid homeostasis in Leydig cells. In addition, *Tspo*-null cells may be at risk for steroidogenic substrate exhaustion [6], which is likely related to the observed sex-specific differences.

Several genetically modified and diet-induced animal models of T2D have been generated [26–28], but until now a stress-induced animal model of T2D was not available. Given that adult-onset diabetes is heterogeneous, with a range of characteristics and underlying disease mechanisms [29], a given animal model can mimic only one or two subsets of the condition. The genetically engineered mice we generated with *Nr5a1*-Cre-mediated TSPO deficiency in steroidogenic cells exhibited sustained hyperglycemia, originating from an adrenal gland defect, and no response to the ACTH challenge. Therefore, this animal model is suitable to study the link between stress response and impaired glucose metabolism in the development of prediabetes and T2D.

The *Tspo* cKO mice with hyperglycemia seems to have lost the basic function (s) of TSPO in regulating mitochondrial membrane potential [2] and steroid biosynthesis, while gaining a consequential effect as a result of adrenal gland impairment [6,12]. In our previous report [6], we showed that mice with *Tspo* depletion in the adrenal gland cortex showed increased epinephrine secretion, which produces an elevation in blood glucose level by stimulating glycogenolysis and gluconeogenesis [30]. Therefore, we propose a working model to explain how *Tspo* deficiency in mice increases epinephrine production by the adrenal glands, stimulating glucose production in the liver and increasing circulating glucose levels (Fig. 4C). We believe that the *Tspo* cKO mouse model may be a useful tool to study downstream effectors of the hypothalamic–pituitary–adrenal axis in the stress response and stress-related diabetes.

5. Conclusions

Generation of steroidogenic cell (adrenal) *Tspo* cKO led to sustained high levels of blood glucose, a hallmark of prediabetes. Considering the relationship between increased levels of the stress hormone epinephrine, observed in these mice, and diabetes, the *Tspo* cKO mice could serve as a new animal model for studying stress-related diabetes.

Conflict of interest statement

The authors declare that there are no potential conflicts of interest regarding the publication of this article.

Author contributions

JF and VP designed the research, analyzed data, and wrote the manuscript. JF performed the experiments. EC assisted in animal dissection, tissue collection, and data analysis.

Funding

This work was supported by the Canadian Institutes of Health Research (grant numbers MOP125983 and PJT148659), a Canada Research Chair in Biochemical Pharmacology, and the John Stauffer Dean's Chair in Pharmaceutical Sciences (University of Southern California).

Transparency document

The Transparency document associated with this article can be found, in online version.

Acknowledgements

We thank the Immunophenotyping and Molecular Imaging Platforms of the Research Institute of McGill University Health Centre (RI MUHC) and N. Laughren and S. Loucao of the animal facility of RI MUHC for help with handling laboratory animals.

Appendix A. Supplementary data

Supplementary data to this article can be found online at https://doi.org/10.1016/j.bbadis.2018.10.022.

References

[1] V. Papadopoulos, M. Baraldi, T.R. Guilarte, T.B. Knudsen, J.J. Lacapere, P. Lindemann, M.D. Norenberg, D. Nutt, A. Weizman, M.R. Zhang, M. Gavish, Translocator protein (18 kDa): new nomenclature for the peripheral-type benzodiazepine receptor based on its structure and molecular function, Trends Pharmacol. Sci. 27 (2006) 402–409.
[2] J. Fan, K. Wang, B. Zirkin, V. Papadopoulos, CRISPR/Cas9-mediated Tspo gene mutations lead to reduced mitochondrial membrane potential and steroid formation in MA-10 mouse tumor Leydig cells, Endocrinology 159 (2018) 1130–1146.
[3] J. Li, V. Papadopoulos, Translocator protein (18 kDa) as a pharmacological target in adipocytes to regulate glucose homeostasis, Biochem. Pharmacol. 97 (2015) 99–110.
[4] P. Gut, B. Baeza-Raja, O. Andersson, L. Hasenkamp, J. Hsiao, D. Hesselson, K. Akassoglou, E. Verdin, M.D. Hirschey, D.Y. Stainier, Whole-organism screening for gluconeogenesis identifies activators of fasting metabolism, Nat. Chem. Biol. 9 (2013) 97–104.
[5] P. Gut, Targeting mitochondrial energy metabolism with TSPO ligands, Biochem. Soc. Trans. 43 (2015) 537–542.
[6] J. Fan, E. Campioli, A. Midzak, M. Culty, V. Papadopoulos, Conditional steroidogenic cell-targeted deletion of TSPO unveils a crucial role in viability and hormone-dependent steroid formation, Proc. Natl. Acad. Sci. U. S. A. 112 (2015) 7261–7266.
[7] K.M. Caron, S.C. Soo, W.C. Wetsel, D.M. Stocco, B.J. Clark, K.L. Parker, Targeted disruption of the mouse gene encoding steroidogenic acute regulatory protein provides insights into congenital lipoid adrenal hyperplasia, Proc. Natl. Acad. Sci. U. S. A. 94 (1997) 11540–11545.
[8] S.H. Kim, M.J. Park, Effects of growth hormone on glucose metabolism and insulin resistance in human, Ann. Pediatr. Endocrinol. Metab. 22 (2017) 145–152.
[9] P. Koska, E. Dojcsak Kiss-Toth, A. Juhasz Szalai, G.L. Kovacs, L. Barkai, O. Racz, B. Fodor, Brain glucose sensing and counterregulatory response to hypoglycaemia, Acta Physiol. Hung. 100 (2013) 133–139.
[10] D.S. Oyer, The science of hypoglycemia in patients with diabetes, Curr. Diabetes Rev. 9 (2013) 195–208.
[11] H. Misu, T. Takamura, H. Takayama, H. Hayashi, N. Matsuzawa-Nagata, S. Kurita, K. Ishikura, H. Ando, Y. Takeshita, T. Ota, M. Sakurai, T. Yamashita, E. Mizukoshi, T. Yamashita, M. Honda, K. Miyamoto, T. Kubota, N. Kubota, T. Kadowaki, H.J. Kim, I.K. Lee, Y. Minokoshi, Y. Saito, K. Takahashi, Y. Yamada, N. Takakura, S. Kaneko, A liver-derived secretory protein, selenoprotein P, causes insulin resistance, Cell Metab. 12 (2010) 483–495.
[12] D.R. Owen, J. Fan, E. Campioli, S. Venugopal, A. Midzak, E. Daly, A. Harlay, L. Issop, V. Libri, D. Kalogiannopoulou, E. Oliver, E. Gallego-Colon, A. Colasanti, L. Huson, E.A. Rabiner, P. Suppiah, C. Essagian, P.M. Matthews, Papadopoulos V. TSPO mutations in rats and a human polymorphism impair the rate of steroid synthesis, Biochem. J. 474 (2017) 3985–3999.
[13] J.M. Fernandez-Real, J.C. Pickup, Innate immunity, insulin resistance and type 2 diabetes, Trends Endocrinol. Metab. 19 (2008) 10–16.
[14] H. Inoue, J. Shirakawa, Y. Togashi, K. Tajima, T. Okuyama, M. Kyohara, Y. Tanaka, K. Orime, Y. Saisho, T. Yamada, K. Shibue, R.N. Kulkarni, Y. Terauchi, Signaling between pancreatic beta cells and macrophages via S100 calcium-binding protein A8 exacerbates beta-cell apoptosis and islet inflammation, J. Biol. Chem. 293 (2018) 5934–5946.
[15] S.S. Rajendran, M. Pharm, N. Santhi, Hormonal Regulation of Blood Glucose, RRVS College of Pharmaceutical Sciences, Sulur, 1979.
[16] K. Morohaku, S.H. Pelton, D.J. Daugherty, W.R. Butler, W. Deng, V. Selvaraj, Translocator protein/peripheral benzodiazepine receptor is not required for steroid hormone biosynthesis, Endocrinology 155 (2014) 89–97.
[17] L.N. Tu, A.H. Zhao, D.M. Stocco, V. Selvaraj, PK11195 effect on steroidogenesis is not mediated through the translocator protein (TSPO), Endocrinology 156 (2015) 1033–1039.
[18] L. Sacca, C. Vigorito, M. Cicala, G. Corso, R.S. Sherwin, Role of gluconeogenesis in epinephrine-stimulated hepatic glucose production in humans, Am. J. Phys. 245 (1983) E294–E302.
[19] M.G. Ziegler, H. Elayan, M. Milic, P. Sun, M. Gharaibeh, Epinephrine and the metabolic syndrome, Curr. Hypertens. Rep. 14 (2012) 1–7.
[20] J.G. Eriksson, C. Osmond, E. Kajantie, T.J. Forsen, D.J. Barker, Patterns of growth among children who later develop type 2 diabetes or its risk factors, Diabetologia 49 (2006) 2853–2858.
[21] S. Johansson, A. Iliadou, N. Bergvall, U. de Faire, M.S. Kramer, Y. Pawitan, N.L. Pedersen, M. Norman, P. Lichtenstein, S. Cnattingius, The association between low birth weight and type 2 diabetes: contribution of genetic factors, Epidemiology 19 (2008) 659–665.
[22] P.L. Hofman, W.S. Cutfield, E.M. Robinson, R.N. Bergman, R.K. Menon, M.A. Sperling, P.D. Gluckman, Insulin resistance in short children with intrauterine growth retardation, J. Clin. Endocrinol. Metab. 82 (1997) 402–406.
[23] D.R. McCance, D.J. Pettitt, R.L. Hanson, L.T. Jacobsson, W.C. Knowler, P.H. Bennett, Birth weight and non-insulin dependent diabetes: thrifty genotype, thrifty phenotype, or surviving small baby genotype? BMJ 308 (1994) 942–945.
[24] D. Mi, H. Fang, Y. Zhao, L. Zhong, Birth weight and type 2 diabetes: a meta-analysis, Exp. Ther. Med. 14 (2017) 5313–5320.
[25] J. Mi, C. Law, K.L. Zhang, C. Osmond, C. Stein, D. Barker, Effects of infant birthweight and maternal body mass index in pregnancy on components of the insulin resistance syndrome in China, Ann. Intern. Med. 132 (2000) 253–260.
[26] A.J. King, The use of animal models in diabetes research, Br. J. Pharmacol. 166 (2012) 877–894.
[27] K. Srinivasan, P. Ramarao, Animal models in type 2 diabetes research: an overview, Indian J. Med. Res. 125 (2007) 451–472.
[28] A. King, J. Bowe, Animal models for diabetes: understanding the pathogenesis and finding new treatments, Biochem. Pharmacol. 99 (2016) 1–10.
[29] E. Ahlqvist, P. Storm, A. Karajamaki, M. Martinell, M. Dorkhan, A. Carlsson, P. Vikman, R.B. Prasad, D.M. Aly, P. Almgren, Y. Wessman, N. Shaat, P. Spegel, H. Mulder, E. Lindholm, O. Melander, O. Hansson, U. Malmqvist, A. Lernmark, K. Lahti, T. Forsen, T. Tuomi, A.H. Rosengren, L. Groop, Novel subgroups of adult-onset diabetes and their association with outcomes: a data-driven cluster analysis of six variables, Lancet Diabetes Endocrinol. 6 (2018) 361–369.
[30] R.S. Sherwin, L. Sacca, Effect of epinephrine on glucose metabolism in humans: contribution of the liver, Am. J. Phys. 247 (1984) E157–E165.